

1 **POPULATION ANALYSIS OF MORTALITY RISK:**
2 **PREDICTIVE MODELS USING MOTION SENSORS FOR**
3 **100,000 PARTICIPANTS IN THE UK BIOBANK NATIONAL COHORT**

4
5 Haowen Zhou^{1,3}, MS, Ruoqing Zhu¹, PhD, Anita Ung², MD, Bruce Schatz^{2,3}, PhD
6 ¹Department of Statistics and ²College of Medicine
7 ³Carl R. Woese Institute for Genomic Biology
8 University of Illinois at Urbana-Champaign, Urbana Illinois 61801 USA
9

10 *Corresponding Author:* Bruce Schatz, Department of Medical Information Science, Institute for
11 Genomic Biology, University of Illinois, Urbana IL 61801 USA schatz@illinois.edu
12

13 **Short Title: Population Analysis of Mortality Risk using Motion Sensors**
14
15

16 **ABSTRACT**
17

18 We have developed novel technology for health monitoring, which inputs motion sensors to
19 predictive models of health status. We have validated these models in clinical experiments with
20 carried smartphones, using only their embedded accelerometers. Using smartphones as passive
21 monitors for population measurement is critically important for health equity, since they are
22 ubiquitous in high-income countries already and will become ubiquitous in low-income countries
23 in the near future. Our study simulates smartphones by using accelerometers as sensor input.

24 We analyzed 100,000 participants in UK Biobank who wore activity monitors with motion
25 sensors for 1 week. This national cohort is demographically representative of the UK population,
26 and this dataset represents the largest such available sensor record. We performed population
27 analysis using walking intensity, with participants whose motion during normal activities
28 included daily living equivalent of timed walk tests. We extract continuous features from sensor
29 data, for input to survival analysis for predictive models of mortality risk.

30 Simulating population monitoring, we validated predictive models using only sensors and
31 demographics. This resulted in C-index of 0.76 for 1-year risk decreasing to 0.73 for 5-year. A
32 minimum set of sensor features achieves similar C-index with 0.72 for 5-year risk, which is
33 similar accuracy to previous studies using methods not achievable with phone sensors. The
34 minimum model uses average acceleration, which has predictive value independent of
35 demographics of age and sex, as does the physical measure of gait speed. Our digital health
36 methods achieve the same accuracy as activity monitors measuring total activity, despite using
37 only walking sessions as sensor input, orders of magnitude less than existing methods.

38

39 **AUTHOR SUMMARY**

40 Supporting healthcare infrastructure requires screening national populations with passive
41 monitors. That is, looking for health problems without intruding into daily living. Digital health
42 offers potential solutions if sensor devices of adequate accuracy for predictive models are
43 already widely deployed. The only such current devices are cheap phones, smartphone devices
44 with embedded sensors. This limits the measures to motion sensors when the phones are carried
45 during normal activities. So measuring walking intensity is possible, but total activity is not.

46 Our study simulates smartphone sensors to predict mortality risk in the largest national cohort
47 with sensor records, the demographically representative UK Biobank. Death is the most definite
48 outcome, accurate death records are available for 100,000 participants who wore sensor devices
49 some five years ago. We analyzed this dataset to extract walking sessions during daily living,
50 then used these to predict mortality risk. The accuracy achieved was similar to activity monitors
51 measuring total activity and even to physical measures such as gait speed during observed walks.
52 Our scalable methods offer a potential pathway towards national screening for health status.

53 INTRODUCTION

54 The association of physical activity with mortality risk is well known. National cohort studies
55 using self-reports have shown intensity is correlated with survival, so persons with lower
56 mortality have more moderate-to-vigorous activity and less sedentary activity [1]. These studies
57 focus upon the volume of activity at certain level of intensity. These have been replicated with
58 large meta-analysis studies using objective physical activity, where wearable sensors record total
59 activity and statistical models predict mortality risk from accelerometer measures [2]. Cohort
60 meta-analysis also shows sensor features improve model performance beyond traditional risk
61 factors [3], e.g. smoking and alcohol, while independent of demographics, e.g. age and sex.

62 Besides quantity of intensity, there are effects of quality of intensity. Physical measurements
63 focus upon walking as moderate activity, in-between vigorous and sedentary. Large meta-
64 analysis studies show gait speed is correlated with mortality risk [4], with timed walking over
65 short distances such as 6 seconds for 4 meters. National cohort studies using self-reports show
66 walking pace is the unique feature beyond traditional risk factors in improving mortality risk for
67 cardiovascular disease [5]. The 6 minute walk test [6], where persons walk steadily in hospital
68 corridor, is a standard evaluation for cardiopulmonary disease. This test has been shown in large
69 meta-analysis studies to be strong independent predictor of mortality from heart failure [7].

70 We analyze the largest national cohort, the UK Biobank [8], where 103,683 participants wore
71 accelerometer devices for 1 week as wrist sensors [9]. Following our previous analysis of a
72 national cohort for physical activity in the US Women's Health Initiative [10], we used raw
73 sensor data during labelled walking sessions to identify characteristic motions for predictive
74 models. This is the first population analysis of walking intensity with mobile sensors, and uses
75 only inputs that could be accurately gathered using only personal smartphones.

76 As surmised from this introduction, there are four primary methods for measuring physical
77 activity. It will be shown later that all these methods achieve roughly the same accuracy for
78 predictive models of mortality risk. Two methods are active, requiring persons explicitly do
79 some activity, such as answering a questionnaire concerning their health status (self-report) or
80 walking fixed distance under observation (gait-speed). These have proven feasible within cohort
81 studies, but are problematic for population health, due to logistic difficulty of getting large
82 numbers of people to perform the required tasks on a routine basis. Two methods are passive,
83 requiring persons to wear measurement devices, such as activity monitors, to measure total
84 activity during the day or specific measures like walking pace over limited periods. These
85 sensor-based methods have the major advantage that they can measure physical activity in daily
86 living, without requiring persons to change their normal activity other than wearing the devices.

87 However, such digital health approaches have had limited success due to problems with health
88 equity. Results with activity monitors are largely from representative samples, such as national
89 cohorts as in this study, rather than from actual large populations. For population measurement
90 in health systems to be routinely available, the measurement devices must be widely deployed
91 [11], which requires mobile phones at present day. In the United States for example, the Pew
92 Research Center estimates 97% of the population has cell phones with 83% having smart phones
93 containing motion sensors [12]. But only 21% of the population has wearable sensors within
94 smart watches or fitness devices [13]. So scalable methods for predictive models using mobile
95 phones would have great impact if limitations can be overcome. Mobile phones are often carried
96 while walking, so could passively capture walking sessions with motion sensors, but rarely
97 carried all day, so not effective to measure total amount of physical activity unlike wearables.

98 The smartphone penetration rate in the United Kingdom, where our dataset was gathered, has
99 increased every year over the past decade, reaching an overall ownership of 92% in 2021. For
100 older adults in the statistical survey [14], less than half of all respondents over the age of 55
101 owned such a device in 2016, but this total rose to 83% in 2021. So adequate devices will soon
102 be everywhere, when the cheapest flip phones have motion sensors. Cheap phones are already
103 widespread worldwide, even in the poorest countries [15]. The global smartphone penetration
104 rate is estimated to have reached over 78 percent in 2020. This is based on 6.4 billion
105 smartphone subscriptions in a global population of 7.8 billion. The global smartphone
106 penetration rate in the general population has great regional variation. In North America and
107 Europe, the smartphone adoption rate stands at roughly 82 and 78 percent, respectively. Whereas
108 in Sub-Saharan Africa, the same rate only stands at 48 percent as of late, showing a roughly 30
109 percent difference in adoption rates between the highest and lowest ranked regions. But note that
110 even in low-income regions, half the population already has smart phones with motion sensors.

111 Since mortality is the definite extreme case of health status, cheap phones could have major
112 impact in addressing health equity if proper models can be developed utilizing only their sensors
113 when they are carried. Our study uses the sensor dataset from the largest current national cohort,
114 the UK Biobank. Although this data was gathered from activity monitors, our sensor models use
115 only the inputs feasible to gather with cheap phones. This is possible because of our extensive
116 clinical experiments with cheap phones, developing highly accurate predictive models for health
117 status with cardiopulmonary patients [16]. The scale of 100K participants provides significant
118 generality to the model results, given that the cohort demographics for all 500K participants in
119 UK Biobank matches the demographics of the national population [17], and their sensor cohort
120 has similarly representative demographics.

121 **RESULTS**

122 We show short bursts of steady walking suffice for predictive models of mortality risk, evaluated
123 using raw sensor data for 100,000 participants in UK Biobank. Our Results evaluate the model
124 accuracy for mortality risk using walking intensity, defined as 12 walking windows of 30
125 seconds each during a consecutive session, representing daily living versions of walk tests. Our
126 accuracy is comparable to previous models using daily profiles of activity volume. Our methods
127 are logistically easier, with 6 minutes per day (12 windows) rather than 600 minutes (10 hours)
128 per day of sensor records. Although the analyzed dataset uses wrist sensors, our previous work
129 showed cheap smart phones have good enough accelerometer sensors to be accurately utilized
130 for similar analysis of walking sessions [18]. Our clinical studies have shown predictive models
131 using only walking intensity can accurately compute pulmonary function for cardiopulmonary
132 patients [16]. Thus our analysis with wearable sensors for predicting mortality is directly
133 applicable for clinical practice with personal smartphones, already ubiquitous in the UK and the
134 US populations, and widespread in global populations.

135

136 **Max (maximum) Models**

137 To model mortality, we consider maximum follow-up time of 1/2/3/4/5 years. This means when
138 the maximum follow-up time is 1 year, any event after 1 year after sensor records is ignored. So
139 we can evaluate model accuracy in early risk years, as well as standard 5-year mortality. The UK
140 Death Registry is used to determine which participants had died by that time.

141 As detailed in the Methods section, we choose 20 traditional predictors, from self reports and
142 laboratory tests. These 20 questions are listed in Table 1 as the Categorical Features. The full
143 encoding from UK Biobank data is given in Supplementary Table S1. We also choose 76 derived

144 predictors from motion (accelerometer) sensors. These 76 sensor features are listed in Table 2 as
145 the Continuous Features. The full encoding from UK Biobank software [19] is given in
146 Supplementary Table S2. We fit a penalized Cox proportional hazard model with all these
147 features, and denote this the *Max Model*, which evaluates accuracy with maximum functionality.
148 Figure 1 gives the computation flowchart for predictive models.

149 We computed Max Models for different groups of categorical features. All the Models
150 included the 3 demographic features (age/sex/race). The continuous variables are all 76 sensor
151 features, with only steady walking as model input. Figure 2 shows that 100,655 participants met
152 the inclusion criteria of 1 walking session of 6 steady minutes during the 1 week. The Max
153 Model plots are shown in Figure 3. The plot showing continuous variables alone is given in
154 Figure 3a, where continuous is a distinct improvement on demographics. The C-index is 0.76 at
155 1-year risk, falling to 0.73 at 5-year risk. The modifiable risk factors are similar at 1-year, where
156 the sensors are more recent, but slightly better at 5-year risk. The advanced disease are
157 significantly better even more at 1-year, but converge to the same as risk factor at 5-year risk.

158 The continuous variables always improve the accuracy of any set of features, as plots show in
159 Figure 3b. Continuous features with demographics only at the bottom is 0.76 at 1-year and 0.73
160 at 5-year. Whereas continuous with all categorical features at the top is 0.83 at 1-year and 0.78 at
161 5-year. In-between, continuous slightly improves the curve for risk factors and the curve for
162 advanced disease. The C-index evaluation numbers of all the Max Models are given in Table 3.

163 Continuous variables have many similarities. Sensor features extracted from signal processing
164 on raw accelerometry compute the same input with similar outcomes on predictive models. Each
165 feature does provide additional accuracy, as shown in Supplementary Table S3, which gives
166 marginal performance of each feature by itself. The top features after Age are ENMOTrunc and

167 MPD, along with their variant computations ENMOabs and MAD. These are features measuring
168 the average acceleration of sensor signal via Euclidean Norm or Mean Deviation. ENMO is
169 Euclidean Norm Minus One, after adjusting acceleration for effects of gravity [20].

170 Lasso models can be utilized to select fewer features, by focusing on those most predictive
171 [21]. The additional discrimination provided by each feature flattens out quickly, so 4 features
172 provide the same model accuracy as all 76 features, for cross-validated C-index. This is shown in
173 Figure 4, which shows cumulative effort of multiple features flattening after 4 features.

174 A Lasso model average hierarchy is displayed in Supplementary Figure S1, with 16 selected
175 features displayed in red. This model uses the optimal lambda selected from cross-validation.
176 The tree is constructed using the hierarchical clustering algorithm to group sensor features, such
177 that features in similar branches of the tree have similar contributions. At the center of the tree
178 are the acceleration magnitude sensor features – enmoTrunc and enmoAbs, plus MAD and MPD.
179 The red ones are stronger, so enmoTrunc and MPD sensor features, among the discriminating
180 ones, are the best candidates for continuous features. These measure mean and standard
181 deviation of average acceleration, shown to be strongly correlated with intensity of activity [22].
182 ENMO uses the magnitude of the acceleration and MxD uses the signal of the accelerometer.

183

184 **Min (minimum) Models**

185 Feature selection implies a parsimonious model might be equally accurate and thus more
186 practical, since requires less input and less compute. Hence, we explore the stepwise model
187 strategy that utilizes small numbers of features. We denote this the *Min Model*, as shown in the
188 flowchart in Figure 1. Such models include demographics and selected continuous features. For
189 practical outcomes, we also include risk factors that are easy to change (especially modifiable),

190 such as smoking and alcohol, health (general) and obesity (BMI). Min Model values are given in
191 Table 4. We rank order the top 10 features, after considering all 76 features.

192 If only selected continuous features are considered, then the cumulative effort on model
193 accuracy is given in Table 4a for this minimum set. The top accelerometer feature is
194 ENMOTrunc, acceleration magnitude correlated with activity intensity, truncated to zero for
195 negative values [22]. With the significant demographic variables Age and Sex, the C-index is
196 0.727 for Min Model, rounding to 0.73, the same as the Max Model. The remaining top 10 had
197 little extra effect, these features include other mean and standard deviation of acceleration.

198 When easy risk factors are also included, acceleration magnitude features improve C-index.
199 As shown in Table 4b for Min Model, health and MPD beat smoking and obesity (BMI). This
200 result is comparable to the UKB mortality study with categorical features only, where the most
201 predictive features were self-reported health and walking pace [23]. The acceleration magnitude
202 sensor features represent an objective passive measure replacing subjective walking pace. With
203 general health included, MPD increases C-index to 0.74 using Mean Power Deviation, while
204 slightly beating the traditional risk factors as did the self-reported walking pace [5].

205

206 **Demographic Independence**

207 For sensor features to provide clinical utility beyond known demographics and easy risk factors,
208 they must provide orthogonal support, for model accuracy independent of demographics.
209 Following the original gait speed study [4], we generated the curves of 98% percentile survival
210 time as functions of ENMOTrunc against Age and Sex. Death events are about 2% of the cohort.
211 These mortality curves are shown in Figure 5, demonstrating sensor measures provide
212 independent value. Higher ENMO values predict longer survival, independent of age and sex.

213 The other acceleration magnitude features (MPD/MAD) have similar independence graphs. So
214 the activity intensity predictor ENMO predicts mortality risk -- higher magnitude is lower risk.

215

216 **Geographic Variation**

217 Over the entire cohort of 100K participants, the predictive model gives 0.73 C-index for 5-year
218 mortality. However, it is worth noting that different populations have different accuracies using
219 the same models. To evaluate this, we computed different statistical models (Lasso, Stepwise),
220 then computed the C-index independently for each assessment center in 22 cities across the UK.
221 Accuracy varies widely, as shown in Supplementary Figure S2. For example, the Lasso model
222 averages 0.77 but ranges from 0.73 to 0.84, Lasso Continuous averages 0.73 but ranges from
223 0.66 to 0.77 C-index. With just Continuous, like the Min Model, Glasgow and Edinburgh have
224 5-year 0.77 C-index. The original mortality study without sensors had its highest reported scores
225 at the Scottish sites as well [23]. Their analysis with categorical features only showed Glasgow
226 and Edinburgh had 0.80 C-index with 13 questions while our categorical only is 0.81 and 0.80
227 with 17 questions that represent a superset of theirs.

228

229 **Intensity versus Volume**

230 As noted, physical activity is traditionally measured by volume profile. So individuals with
231 lower mortality have more moderate-to-vigorous activity and less sedentary activity. That is, the
232 duration of activity is considered more important than the intensity itself. These measurement
233 concepts for physical activity are international standards [24]. Such studies of physical activity
234 commonly utilize wearable sensors since they are specific measures within limited periods [2].
235 The participants can thus be relied upon to wear the devices all day, so the studies assume 10
236 hours per day of wear time during normal activities. For effective usage in daily living, the

237 patients must continuously wear a medical quality sensor device. In contrast, our methods
238 assume a single 6MWT per day, so 6 minutes rather than 600 minutes, two orders of magnitude
239 less sensor data. Our methods enable the usage of cheap smart phones, since often carried while
240 walking yet having adequate accelerometers for predictive models of pulmonary function [16].

241 With cardiopulmonary patients, intensity is more important than duration, as shown in large
242 meta-analysis studies [25]. Our model prediction relies upon walking intensity in short bursts
243 being an effective surrogate for activity intensity over whole days. Intuitively, walking is the
244 unique physical activity, which ranges in intensity from vigorous (fast) to sedentary (slow). Brisk
245 walks are nearly as vigorous as running and shuffling walks are nearly as sedentary as standing.

246 Another confirmation of walking intensity as an effective surrogate for activity volume is
247 shown by our Lasso model average hierarchy in Supplementary Figure S1, with the most
248 discriminating selected sensor features displayed in red. The center of the tree is the acceleration
249 magnitude features such as ENMO and MPD. In a single central branch for selected features are
250 MCR, Mean Crossing Rate, along with MMCR (Maximum and Minimum average Crossing
251 Rate), the closest equivalent with walking intensity to RA (Relative Amplitude) which measures
252 activity volume, as described below. In addition to overall average for MMCR, nearby branches
253 include in red, the specific yMMCR and zMMCR due to walking motions. But the other 4
254 features in red near the center are the equivalents of RA for short bursts, which we computed for
255 comparative purposes as special additions to biobank features. These concern the crossing rate,
256 how often the acceleration changes from above the mean to below the mean and vice versa,
257 which we previously utilized for predictive models of fall risk in national cohorts [10].

258

259

260

261 **Comparing Accuracy to Concurrent Study**

262 The UK Biobank accelerometer dataset has also been analyzed by a concurrent study which used
263 cooked data to analyze the activity volume [26], rather than using the raw data as we did to
264 analyze the walking intensity. This study took the 5 second averages from Biobank field 90004
265 and further averaged over 1 minute intervals. Our study used raw signals from field 90001,
266 which can detect characteristic motions of walking intensity, since 1 minute contains 6000 data
267 points rather than only 1. Our Min Model achieves the same C-index accuracy of 0.72 as their
268 study for continuous features with demographics, although their analogue of ENMOtrunc called
269 Relative Amplitude requires 100 times more minutes per day. (RA compares the highest 10
270 hours of activity to the lowest 5 hours, so need 600 minutes rather than 6 per day). Since they are
271 measuring volume (quantity) of physical activity, they average the sensor records to 1 value per
272 minute of accelerometer data. Since we are measuring intensity (quality) of physical activity, we
273 use the raw data at 100 Hz which is 6000 values per minute. So each day, we measure 100 times
274 less minutes with 10 times more samples. Due to their requirement of at least 3 days with at least
275 10 hours per day sensor records, they excluded 21K participants while we excluded 3K
276 participants, so we have 7 times more inclusions for measured participants.

277 Given the geographic variation, we could focus solely upon the highest accuracy at the
278 Scottish sites of Glasgow and Edinburgh, as did the original UK Biobank mortality study using
279 self-reported questionnaires only. There we achieve 5-year 0.77 C-index with the Min Model.
280 This is 5 points higher than the concurrent study using activity volume, despite using 30 minutes
281 instead of 30 hours of sensor input, per participant per week of sensor measure. In considering
282 the Max Model with categorical as well as continuous features, the concurrent study listed
283 similar categorical features to ours but did not explain the derivation. We give the Biobank

284 fields used to extract our categorical features in Supplementary Table S1, with summary
285 statistics for participants and values.

286 In our study, we used Date fields giving physician consensus for disease diagnosis, more
287 detailed from more sources than the participant self reported answers used in the concurrent
288 study. This enables a fair comparison between categorical and continuous features, both up to
289 date at the time of sensor records. The self reported disease features are from participant
290 registration, which is 6 years before the sensor records (2008 versus 2014). So their sensor
291 features are more recent than their categorical features, and hence more accurate for mortality
292 prediction than is actually correct, similar to 5-year versus 10-year mortality risk. Their
293 conclusion that objective measures with sensor features improve prediction performance of risk
294 factors thus may be flawed, a confounded artifact of when data was gathered.

295

296

297 **DISCUSSION**

298 Measuring activity via walking intensity has become standard practice for clinical visits, where
299 gait speed measures short walks. Detailed meta-analysis showed gait speed independent of
300 age/sex [4], with pooled C-index close to 0.72 model accuracy for 5-year risk. Objective
301 physical activity (OPA) measures the “quantity” of physical activity, such as total amount of
302 moderate-to-vigorous physical activity. This requires sensor devices be worn all day, so a
303 concurrent study [26] of the UK Biobank sensor dataset showed the highest predictor was
304 relative amplitude (RA), ratio of most active 10 hours of average acceleration to least active 5
305 hours. The C-index was 0.72, with RA plus age/sex for 5-year risk, based upon 600 minutes per
306 day of sensor records.

307 A walk test measures “quality” (intensity) rather than “quantity” (volume). Our previous work
308 showed accelerometer sensors in carried smartphones can digitally model physical distance [27]
309 and oxygen saturation [28] from Six Minute Walk Test (6MWT). We also showed the
310 pulmonary models similarly worked with carried smartphones during daily living [16]. The
311 logistic advantage of 6 minutes walking intensity is two orders of magnitude less frequent sensor
312 input, using ENMO for quality versus RA for quantity. This makes it possible to effectively
313 utilize smart phones instead of wearable sensors for predictive models.

314 The Min Model with fewer sensor features holds at the same 0.72 for 5-year risk. Using
315 continuous features only without categorical features, our Max Model yields 0.73 C-index for 5-
316 year risk, with greater accuracy in earlier years yielding 0.76 for 1-year risk. We note model
317 accuracy varies by local sites, as shown in Supplementary Figure S2, with 0.77 for 5-year at
318 Glasgow and Edinburgh, where the original mortality study using self reports also did best [23].
319 Our digital measures of walking intensity are better in quality for predictive power versus
320 traditional modifiable risk factors such as smoking and obesity. This objective result confirms
321 the previous subjective UK Biobank study using self reports of walking pace [5].

322 We are involved in planning the physical activity study for the US Precision Medicine
323 Initiative (All of Us Research Program). This cohort is projected to become the largest national
324 cohort with more than 1M participants, close to half already registered. These participants are
325 being recruited to be representative of the national population, which is far more diverse in the
326 US than in the UK. All agreeing participants would be longitudinally measured on their personal
327 smartphones, both larger and longer than our mortality study as well as directly utilizing phone
328 sensors for the measurement study.

329

330 Our previous work showed accelerometer motion sensors in cheap smart phones can capture
331 equivalent model input for gait analysis as expensive medical devices. This is particularly
332 important for health equity purposes, given populations at highest health risk are often the most
333 under-resourced—persons most likely to have cheap phones rather than wearable devices would
334 benefit most from easy assessment. Phone apps could record six minutes of consecutive walking
335 during daily living, then compute predictive models for risk stratification via population analysis
336 [11]. Major cohort studies using self reported status have shown that cardiovascular health is
337 strongly correlated with physical activity, largely independent of the socioeconomic level of the
338 country of the participants [29]. Thus our results from high-income countries may well be
339 directly applicable to low-income countries as well. Healthy longevity could be facilitated for all
340 adults possessing cheap phones, using the minimum model to assess gait status, computed on
341 their phones for the maximum privacy. Implementing effective healthcare infrastructure requires
342 continued research into screening populations with ubiquitous sensors [30].

343

344

345 **MATERIALS AND METHODS**

346 **Ethics Statement**

347 This study analyzes datasets provided by UK Biobank, with subjects identified only by
348 participant number. This Biobank is a national resource in the United Kingdom, providing
349 datasets to international researchers who have approved projects. Our project entitled
350 “Predictive Models of Mortality Risk from Passive Monitors measuring Physical Activity” is
351 approved with ID 45178. This enabled us to download datasets with selected portions of their
352 complete database, each dataset was approved by the Biobank as was each investigator including

353 all of the authors. UK Biobank supports extensive human subjects protection including written
354 informed consent from each participant. The signed Materials Transfer Agreement between
355 University of Illinois and UK Biobank specifies that we will abide by all their ethical standards.

356

357 **Study Participants**

358 UK Biobank is a prospective study with over 500,000 participants aged 40-69 years [8]. These
359 participants were recruited during 2006-2010 from 22 assessment centers throughout the UK.
360 The study is longitudinally collecting participants' information, including data from
361 questionnaires (self reports), physical measures (laboratory tests), and accelerometers (sensor
362 records). It is representative of the national population for demographic and geographic
363 considerations, although the entire cohort shows less disease and more education than the UK
364 population at large [17]. Within the entire cohort, traditional risk factor associations agree for
365 mortality outcomes with nationally representative cohort studies [31]. Thus the cohort dataset
366 for sensor analysis is uniquely suitable for predictive models. UK Biobank provides accurate
367 datasets for sensor input with physical activity and status output with health outcomes [19].

368 Our study focuses on the subset of 103,683 participants who agreed to wear a wrist-worn
369 triaxial accelerometer, an Axivity AX3 sampling at 100Hz, continuously for 1 week [9]. These
370 participants were aged 45-79 when data was collected in 2013-2015. We implemented
371 inclusion/exclusion criteria shown in Figure 2. We exclude 257 participants for insufficient
372 device wear time. Our analysis focused on walking intensity, so participants must have sufficient
373 length of steady walking, as defined below. The Biobank software [19] divides sensor data into
374 non-overlapping 30-second windows with activity labels. The Biobank software divides sensor
375 data into non-overlapping 30-second windows with activity labels. These are highly accurate,

376 due to careful derivation from training set of representative participants who wore head-mounted
377 cameras to visually identify activities. We included any participant with at least one session of
378 steady walking, defined by 12 consecutive walking windows. Only windows labelled as walking
379 were considered input data for feature extraction. We exclude 2758 participants for insufficient
380 walking, which with other minor exclusions, yields total 100,655 participants for our analysis.
381 There were 2048 included deaths from UK Biobank field 40023, derived from the National
382 Death Registry, which is a comprehensive curated dataset. We analyzed all-cause 5-year
383 mortality, with sensor records from Jun 2013 to Dec 2015 and deaths until Dec 2019 to avoid
384 COVID-19. For highest accuracy, our analysis used all qualifying participants, after trying
385 different subsets including different age ranges.

386

387 **Steady Walking in Daily Living**

388 Walk tests are widely used to clinically evaluate status of cardiopulmonary patients. A standard
389 assessment is the Six Minute Walk Test (6MWT), where a patient walks back and forth in a
390 corridor for six minutes and their walked distance indicates their health status [6]. With COPD
391 patients, this period is long enough so patients slow down in correlation with their status
392 determined by spirometry [32]. Such walk tests are also used for CHF patients [33], who also
393 exhibit Shortness of Breath on Exertion (SOBOE) [34]. We have previously shown with such
394 cardiopulmonary patients that accelerometer sensors can measure slowdown/speedup with
395 clinical accuracy, for predictive models of 6MWT distance and pulmonary function [27,16].
396 These were clinical experiments with COPD/CHF patients who performed 6MWT in hospital
397 rehabilitation, with carried smartphones recording accelerometer sensors.

398 There is no current standard for walk tests during daily living. We chose 6 minutes as
399 empirical lower bound for cardiopulmonary slowdown during *steady walking*, with relaxed
400 criteria to allow longer periods. During daily living, a person may walk more slowly than when
401 they are pushing hard during walk test, so it might take longer for them to experience SOBOE.
402 Thus we require 12 consecutive walking windows to be the “equivalent of 6MWT”, and include
403 all such labelled windows for included participants with at least 1 such session. For example, 4
404 consecutive walking windows would be excluded, while 12 consecutive windows or even 20
405 would be included. All participants had 1 session of 6 minutes continuous walking during the 1
406 week, although only 10% walk half an hour in 6 minute sessions as shown in Figure 6.

407

408 **Mortality Predictors: Traditional Categorical and Accelerometer Continuous**

409 UK Biobank collected questionnaires during 2006-2010, when participants registered. We
410 extract categorical features based upon self-reported answers and laboratory tests. We select 20
411 questions to characterize health status, including 7 Advanced Disease Conditions, 10 Modifiable
412 Risk Factors, 3 Demographics. These are grouped into categories in Table 1. The original
413 analysis for mortality risk using only categorical features found 13 features to be most
414 discriminating [23], our list includes theirs. Supplementary Table 1 gives summary statistics.

415 Accelerometer data is collected by Axivity AX3 wrist-worn accelerometer, which collects
416 100Hz triaxial signals [9]. We follow the provided Biobank methods to extract features from
417 raw data [19]. Our previous work showed raw sensor data was needed to predict status of
418 pulmonary function in clinical studies with cardiopulmonary patients [16]. Model input was
419 6MWT sensor records, so more data points are needed than simply average sensor data over a
420 labelled walking window.

421 Every 30 second time window is an epoch for measuring physical activity with single label,
422 yielding 3000 3D acceleration points. The total number of possible epochs over 7 days is 20160.
423 In each epoch, we extract a 76-dimensional feature vector, where each feature describes certain
424 characteristics of motion patterns. Signal features are derived from time domain and frequency
425 domain [35,36]. We use only features from time domain, since measuring walking intensity over
426 time periods. We used 38 features from the Biobank software time domain [19], and computed
427 another 38 features from their frequency domain following our previous work [16]. The 76
428 sensor features are listed in Table 2, while Supplementary Table 2 gives their formulas.

429 We added dimensional data, such as x-y-z, plus computing our own features from the
430 frequency domain of Biobank software¹³. Our new features include those useful in other studies.
431 These included RMS (root mean square) from our prior work [16], which is computable from
432 FFT. Total activity count (TAC) is the overall feature provided by commercial fitness devices
433 such as research standard Actigraph GTX-3. We computed comparisons of most active periods
434 to least active, such as MMCR (Maximum and Minimum average Cross Rate) and MCR (Mean
435 Cross Rate), similar to physical activity profiles from activity volume methods. Full formulas for
436 sensor features are given in Supplementary Table 2. The major features are defined in terms of
437 ENMO, mean acceleration correlated with activity intensity such as walking versus standing.
438 These include MPD and MAD, Mean Power Deviation and Mean Amplitude Deviation of
439 accelerometer magnitude signals [37].

440

441 **Sensor Data Processing**

442 The raw data was collected into 30-second windows over the entire week of recording, each
443 window contained 3000 3-axis motion samples from field 90001. This comprised 25 terabytes.

444 We analyzed this dataset using the Biocluster2 at the Carl R. Woese Institute for Genomic
445 Biology, which has 72 nodes of Xeon Gold 6150s with 2 cores each of 2.7 GHz and 4GB
446 memory. We computed 1037 batches of instances, where each batch consists of 100 instances.
447 These instances covered the participant sensor record for each of almost 103,700 participants.

448 The total processing time for feature extraction was 3100 hours of compute time. It takes
449 about 3 hours for each node to process each batch. The typical sensor processing used 50 nodes
450 on the shared cluster, so the total real time was about 62 hours, or about 3 days. The steady state
451 of extracted features is 1.2 TB, which we kept on the cluster storage as input to run the models.

452

453 **Mortality Prediction Models and Survival Function Estimation**

454 The prediction response is the time interval between end time of participant mortality and device
455 wearing for sensor record. Since the outcome is time-to-event and subject to censoring, we
456 utilize survival analysis [38]. Hence we consider the Cox proportional hazard model [39] and its
457 penalized version [40]. We use the elastic net penalty [41], which consists of both l1 and l2
458 penalties of the coefficients, controlled by two tuning parameters α and λ . The method is
459 implemented using the R package glmnet [42]. To select the optimal tuning, we consider $\alpha = 0$,
460 0.5, 1 and use a grid of λ values automatically selected by the glmnet package.

461 We then perform 10-fold cross-validation [43]. Cross-validation procedures are more stable
462 than pre-fixing testing data since they enable all observed data to be used in evaluation steps.
463 These are commonly used in data analytic procedures with machine learning methods [44]. The
464 procedure 10-fold is the averaged result of performing 10 such pre-fixing procedures. In contrast,
465 results derived from pre-fixing the testing data only once can be greatly effected by the
466 randomness involved in choosing the test set.

467 We use a stratified 10-fold cross-validation approach, since the proportion of death is small
468 (about 2% of participants). For each model with maximum follow-up length (1/2/3/4/5 years),
469 we consider the data is randomly split into 10 equal-sized subsets. Each subset contains 1/10 of
470 the live data (participants who are still alive or censored by the maximum follow-up time) and
471 1/10 of the dead data (participants who have died by the maximum follow-up time). With these
472 10 equal-size datasets, a single subset is utilized for testing the model and the remaining 9
473 subsets are used as training data. The cross-validation process is repeated 10 times with every
474 subset used exactly once as the testing data. Finally, the 10 results from the folds can be
475 averaged to produce a single estimation for a specific model with exact α and λ .
476 For each α , the λ with best performance is selected from grid as model parameter.

477 In addition to the regularized Cox proportional hazards model, we fit other models to compare
478 their performance. We adopt stepwise selection to choose variables. With fixed variables as
479 input, we set the prediction performance as inclusion criteria to do stepwise forwards selecting
480 over these variables. In every step, the variable that increases the C-index the most based on the
481 previous selected variables is included in the group. The selection runs until the increment is less
482 than a specific threshold. We have tested over traditional predictors and accelerometer derived
483 predictors with threshold 0.01 and 0.001, to enable model evaluation.

484 The Concordance Index (C-index) is used to evaluate the model performance [45]. The C-
485 index can be interpreted as the fraction of all pairs of subjects whose predicted survival times are
486 correctly ordered as the observed survivals, while correcting for censoring. Hence, it is more
487 sensible than other common criteria such as the overall accuracy or the Area under the Curve.

488

489 **ACKNOWLEDGEMENTS**

490 Qian Cheng at Salesforce AI Research advised us on predictive models of wearable sensors.

491 **REFERENCES**

- 492 1. Wang Y, Nie J, Ferrari G, Rey-Lopez JP, Rezende LFM. Association of Physical Activity
493 Intensity with Mortality: A National Cohort Study of 403,681 US Adults. *JAMA Intern Med*
494 2021 (Feb);181(2):203-211.
- 495 2. Ekelund U, Tarp J, Fagerland M, et al. Joint associations of accelerometer measured physical
496 activity and sedentary time with all-cause mortality: a harmonised meta-analysis in more than
497 44,000 middle-aged and older individuals. *Br J Sports Med* 2020 (Dec);54(24):1499-1506.
- 498 3. Tabacu L, Ledbetter M, Leroux A, Crainiceanu C, Smirnova E. Quantifying the Varying
499 Predictive Value of Physical Activity Measures Obtained from Wearable Accelerometers on All-
500 Cause Mortality over Short to Medium Time Horizons in NHANES 2003-2006. *Sensors (Basel)*
501 2020 (Dec);21(1):4 (19pp).
- 502 4. Studenski S, Perera S, Patel K, et al. Gait speed and survival in older adults. *JAMA* 2011
503 (Jan);305(1):50-58.
- 504 5. Argyridou S, Zaccardi F, Davies M, Khunti K, Yates T. Walking pace improves all-cause and
505 cardiovascular mortality risk prediction: A UK Biobank prognostic study. *Eur J Prev Cardiol*
506 2020 (Jul);27(10):1036-1044.
- 507 6. ATS Committee on Proficiency Standards for Clinical Pulmonary Function Laboratories. ATS
508 statement: guidelines for the six-minute walk test. *Am J Respir Crit Care Med* 2002
509 (Jul);166(1):111-117.
- 510 7. Grundtvig M, Eriksen-Volnes T, Ørn S, Slind EK, Gullestad L. 6 min walk test is a strong
511 independent predictor of death in outpatients with heart failure. *ESC (Eur Soc Cardio) Heart Fail*
512 2020 (Oct);7(5):2904-2911.

- 513 8. Sudlow C, Gallacher J, Allen N, et al. UK Biobank: an open access resource for identifying
514 the causes of a wide range of complex diseases of middle and old age. PLoS Med 2015
515 (Mar);12(3):e1001779 (10pp).
- 516 9. Doherty A, Jackson D, Hammerla N, et al. Large Scale Population Assessment of Physical
517 Activity Using Wrist Worn Accelerometers: The UK Biobank Study. PLoS One 2017
518 (Feb);12(2):e0169649 (14pp).
- 519 10. Hua A, Quicksall Z, Di C, Motl R, LaCroix AZ, Schatz BR, Buchner DM. Accelerometer-
520 based predictive models of fall risk in older women: a pilot study. Nature (NPJ) Digital Med
521 2018 (Jul);1:25 (8pp). <https://doi.org/10.1038/s41746-018-0033-5>.
- 522 11. Schatz BR. Population measurement for health systems. Nature (NPJ) Digital Med 2018
523 (Jan); 1:4 (4pp). <https://doi.org/10.1038/s41746-017-0004-2>.
- 524 12. Pew Research Center. Demographics of Mobile Devices: Mobile Fact Sheet, 2021 (Apr 7).
525 <https://www.pewresearch.org/internet/fact-sheet/mobile/>.
- 526 13. Pew Research Center. About one-in-five Americans use a smart watch or fitness tracker.
527 2020 (Jan 9). [https://www.pewresearch.org/fact-tank/2020/01/09/about-one-in-five-americans-
528 use-a-smart-watch-or-fitness-tracker/](https://www.pewresearch.org/fact-tank/2020/01/09/about-one-in-five-americans-use-a-smart-watch-or-fitness-tracker/).
- 529 14. O’Dea S. Smartphone ownership in the United Kingdom (UK) 2012-2021. 2021 (May 21).
530 [https://www.statista.com/statistics/271851/smartphone-owners-in-the-united-kingdom-uk-by-
531 age/](https://www.statista.com/statistics/271851/smartphone-owners-in-the-united-kingdom-uk-by-age/).
- 532 15. O’Dea S. Global smartphone penetration rate as share of population from 2016 to 2020.
533 2021 (Dec 16). [https://www.statista.com/statistics/203734/global-smartphone-penetration-per-
534 capita-since-2005/](https://www.statista.com/statistics/203734/global-smartphone-penetration-per-capita-since-2005/).

- 535 16. Cheng Q, Juen J, Bellam S, et al.. Predicting Pulmonary Function from Phone Sensors.
536 Telemed J E Health. 2017 (Nov);23(11):913-919.
- 537 17. Fry A, Littlejohns TJ, Sudlow C, et al. Comparison of Sociodemographic and Health-Related
538 Characteristics of UK Biobank Participants with Those of the General Population. Am J
539 Epidemiol 2017 (Nov);186(9):1026-1034.
- 540 18. Juen J, Cheng Q, Schatz B. A natural walking monitor for pulmonary patients using mobile
541 phones. IEEE J Biomed Health Inform 2015 (Jul);19(4):1399-405.
- 542 19. Willetts M, Hollowell S, Aslett L, Holmes C, Doherty A. Statistical machine learning of
543 sleep and physical activity phenotypes from sensor data in 96,220 UK Biobank participants. Sci
544 Rep 2018 (May);8(1):7961 (10pp).
- 545 20. van Hees VT, Gorzelniak L, Dean León EC, et al. Separating movement and gravity
546 components in an acceleration signal and implications for the assessment of human daily
547 physical activity. PLoS One 2013 (Apr);8(4):e61691 (10pp).
- 548 21. Tibshirani R. Regression shrinkage and selection via the lasso. J Royal Statistical Soc: Series
549 B Methodological 1996;58(1):267-288.
- 550 22. Bakrania K, Yates T, Rowlands AV, et al. Intensity Thresholds on Raw Acceleration Data:
551 Euclidean Norm Minus One (ENMO) and Mean Amplitude Deviation (MAD) Approaches.
552 PLoS One 2016 (Oct);11(10):e0164045 (16pp).
- 553 23. Ganna A, Ingelsson E. 5 year mortality predictors in 498,103 UK Biobank participants: a
554 prospective population-based study. Lancet 2015 (Aug);386(9993):533-540.
- 555 24. Wang R, Bishwajit G, Zhou Y, et al. Intensity, frequency, duration, and volume of physical
556 activity and its association with risk of depression in middle- and older-aged Chinese: Evidence

557 from the China Health and Retirement Longitudinal Study, 2015. PLoS One 2019
558 (Aug);14(8):e0221430 (16pp).

559 25. Laursen AH, Kristiansen OP, Marott JL, et al. Intensity versus duration of physical activity:
560 implications for the metabolic syndrome. A prospective cohort study. BMJ Open
561 2012;2:e001711. doi:10.1136/bmjopen-2012-001711.

562 26. Leroux A, Xu S, Kundu P, et al. Quantifying the Predictive Performance of Objectively
563 Measured Physical Activity on Mortality in the UK Biobank. J Gerontol: A Biol Sci Med Sci
564 2021 (Jul) 13; 76(8):1486-1494.

565 27. Juen J, Cheng Q, Prieto-Centurion V, Krishnan JA, Schatz B. Health monitors for chronic
566 disease by gait analysis with mobile phones. Telemed J E Health. 2014 (Nov);20(11):1035-1041.

567 28. Cheng Q, Juen J, Hsu-Lumetta J, Schatz B. Predicting Transitions in Oxygen Saturation
568 Using Phone Sensors. Telemed J E Health 2016 (Feb);22(2):132-137.

569 29. Lear S, Hu W, Rangarajan S, et al. (2017) The effect of physical activity on mortality and
570 cardiovascular disease in 130,000 people from 17 high-income, middle-income, and low-income
571 countries: the PURE study. Lancet 390: 2643-2653 (Dec 16, 2017).

572 30. Schatz BR, Berlin RB. *Healthcare Infrastructure: Health Systems for Individuals and*
573 *Populations*. London: Springer-Verlag Series in Health Informatics, 2011.

574 31. Batty GD, Gale CR, Kivimäki M, Deary IJ, Bell S. Comparison of risk factor associations in
575 UK Biobank against representative, general population based studies with conventional response
576 rates: prospective cohort study and individual participant meta-analysis. BMJ 2020 (Feb);
577 368:m131. doi: 10.1136/bmj.m131.

578 32. Lahousse L, Verlinden VJ, van der Geest JN, et al. Gait patterns in COPD: the Rotterdam
579 Study. Eur Respir J 2015 (Jul);46(1):88-95.

- 580 33. Jehn M, Schmidt-Trucksäss A, Schuster T, et al. Accelerometer-based quantification of 6-
581 minute walk test performance in patients with chronic heart failure: Applicability in
582 telemedicine. *J Card Fail* 2009;15:334–340.
- 583 34. Clark AL. Origin of symptoms in chronic heart failure. *Heart*. 2006 (Jan);92(1):12-6.
- 584 35. Zhang S, Rowlands AV, Murray P, Hurst TL. Physical activity classification using the
585 GENEa wrist-worn accelerometer. *Med Sci Sports Exer* 2012 (Apr);44(4):742-748.
- 586 36. Ellis K, Kerr J, Godbole S, Staudenmayer J, Lanckriet G. Hip and Wrist Accelerometer
587 Algorithms for Free-Living Behavior Classification. *Med Sci Sports Exerc* 2016
588 (May);48(5):933-940.
- 589 37. Marin F, Lepetit K, Fradet L, Hansen C, Ben Mansour K. Using accelerations of single
590 inertial measurement units to determine the intensity level of light-moderate-vigorous physical
591 activities: Technical and mathematical considerations. *J Biomech* 2020 (Jun);107:109834 . doi:
592 10.1016/j.jbiomech.2020.109834. Epub 2020 May 12.
- 593 38. Fleming TR, Harrington DP. *Counting Processes and Survival Analysis*. Wiley-Interscience,
594 2013, 2nd ed.
- 595 39. Cox DR. Regression models and life tables (with discussion). *J Royal Statistical Soc*
596 1972;34(2):187-220.
- 597 40. Simon N, Friedman J, Hastie T, Tibshirani R. Regularization paths for Cox’s proportional
598 hazards model via coordinate descent. *J Statistical Software* 2011 (Mar);39(5):1.
- 599 41. Zou H, Hastie T. Regularization and variable selection via the elastic net. *J Royal Statistical*
600 *Soc: Series B Methodological* 2005 (Apr);67(2):301-320.
- 601 42. Friedman J, Hastie T, Tibshirani R. Regularization paths for generalized linear models via
602 coordinate descent. *J Statistical Software* 2010;33(1):1.

603 43. Kohavi R. A study of cross-validation and bootstrap for accuracy estimation and model
604 selection. In Ijcai 1995 (Aug 20);14(2):1137-1145.

605 44. Hastie T, Tibshirani R, Friedman J. *The Elements of Statistical Learning: Data Mining,*
606 *Inference, and Prediction*. New York: Springer Series in Statistics, 2016, 2nd ed.

607 45. Harrell FE, Califf RM, Pryor DB, Lee KL, Rosati RA. Evaluating the yield of medical tests.
608 JAMA 1982 (May) 14;247(18):2543-2546.

609

610 **FIGURE and TABLE legends**

611	Table 1	Categorical Features from UK Biobank dataset fields.
612	Table 2	Continuous Features from Participant Sensor Records.
613	Figure 1	Model Flowchart. Which Inputs used for Which Models.
614	Figure 2	Participant Flowchart. Inclusion/Exclusion for Mortality Prediction.
615	Figure 3	Max Model plots with Demographics and Features curves.
616	Table 3	Max Model results with C-index, Feature Sets versus Risk Years.
617	Figure 4	Feature Selection with diminished returns leading to Min Model.
618	Table 4	Min Model results sensor only, with Cumulative C-index rankings.
619	Figure 5	Demographic Independence Curves for sensor records.
620	Figure 6	Walking Distribution of Labelled Sessions during Daily Living.

621
622
623

624 **SUPPLEMENTARY FIGURES/TABLES**

625	Table S1	Categorical Encoding. Features from cohort dataset of 100,655 participants.
626	Table S2	Continuous Encoding. Formulas for Accelerometer Derived Sensor Features.
627	Table S3	Marginal Performance of Top 30 of All Features ranked by C-index.
628	Figure S1	Lasso Model. Hierarchy tree average with red selected features.
629	Figure S2	Geographic Variation of Models across Cohort sites.

630

POPULATION ANALYSIS OF MORTALITY RISK: PREDICTIVE MODELS USING MOTION SENSORS FOR 100,000 PARTICIPANTS IN THE UK BIOBANK NATIONAL COHORT

Haowen Zhou^{1,3}, MS, Ruoqing Zhu¹, PhD, Anita Ung², MD, Bruce Schatz^{2,3}, PhD

¹Department of Statistics and ²College of Medicine

³Carl R. Woese Institute for Genomic Biology

University of Illinois at Urbana-Champaign, Urbana Illinois 61801 USA

medRxiv preprint doi: <https://doi.org/10.1101/2022.04.20.22274067>; this version posted April 21, 2022. The copyright holder for this preprint (which was not certified by peer review) is the author/funder, who has granted medRxiv a license to display the preprint in perpetuity. It is made available under a [CC-BY 4.0 International license](#).

FIGURES/TABLES CONCISE CAPTIONS

Table 1	Categorical Features
Table 2	Continuous Features
Figure 1	Model Flowchart
Figure 2	Participant Flowchart
Figure 3	Max Model plots
Table 3	Max Model values
Figure 4	Feature Selection
Table 4	Min Model values
Figure 5	Demographic Independence
Figure 6	Walking Distribution

Table 1. Categorical Features

ADC Advanced Disease Condition is 7 features (4 Diagnosis + 3 Medicalcare)

MRF Modifiable Risk Factors is 10 features (4 Screening + 3 Habit + 3 Lifestyle)

Demographics

Age/Sex/Race

Age=DateSensorWear-YearOfBirth
Sex=Male/Female, Race=Other/White

Diagnosis

Cardiovascular Disease

Myocardial Infarction, Angina Pectoris

Stroke Cerebral Infarction, StrokeOther

Pulmonary Disease

Cancer

Diabetes

combine 8 fields, eliminate duplicate participants.

Congestive Heart Failure, Ischemic Heart Disease

Stenosis Precerebral Arteries, Cerebral Arteries

Chronic Obstructive Pulmonary Disease (COPD)

Date Diagnosed with Malignant Behavior

combine 3 fields, Type 1 + Type 2 + Other

medRxiv preprint doi: <https://doi.org/10.1101/2022.04.20.22274067>; this version posted April 21, 2022. The copyright holder for this preprint (which was not certified by peer review) is the author/funder, who has granted medRxiv a license to display the preprint in perpetuity. It is made available under a [CC-BY 4.0 International license](https://creativecommons.org/licenses/by/4.0/).

Medicalcare

Operation

Hospital Admissions

Falls

Major Operation for Male + Female

Emergency Admission, Elective Admission

Falls in Last Year, High risk / Low risk

Screening

Hypertension

Cholesterol

Obesity

Medications

Essential Hypertension from Physician Panel

Total Cholesterol, Normal \leq 5.9

Body Mass Index (BMI), Normal $<$ 30

Number of meds, Good $<$ 5

Habit

Alcohol (Intake Frequency)

Smoking (Current Tobacco)

Stress (Illness/Injury/Grief)

Daily, 3-4/Week, 1-2/Week, 1-3/Month, Special,
Never

Yes (Bad), Occasional, No (Good)

Serious Yourself (Bad), Serious Other,
None (Good)

Lifestyle

Health (Overall General Health)

Education (Schooling/Training)

Income (Average Household)

Excellent/Good/Fair/Poor

None = 1 ; Any value (college, professional)

0-18K, 18-31K, 31-52K, 52-100K, >100K Pound/Yr

Table 2. Continuous Features on Sensor Records

76 Variables for Sensor Features: Accelerometer Derived in Time Domain

38 computed using Biobank software on field 90001

38 further derived using Biobank frequency domain

Biobank software: enmoTrunc, mean/sd+x/y/z (9)

MAD/MPD, kurt/skew (4)

Min/Max, 25thp/Median/75thp, autocorr/coefvariation (7)

Range x/y/z, Cov yz/xz/xy, corr yz/xz/xy (9)

pitch/roll/yaw g/sd/avg (9)

medRxiv preprint doi: <https://doi.org/10.1101/2022.04.20.22274067>; this version posted April 21, 2022. The copyright holder for this preprint (which was not certified by peer review) is the author/funder, who has granted medRxiv a license to display the preprint in perpetuity. It is made available under a [CC-BY 4.0 International license](https://creativecommons.org/licenses/by/4.0/).

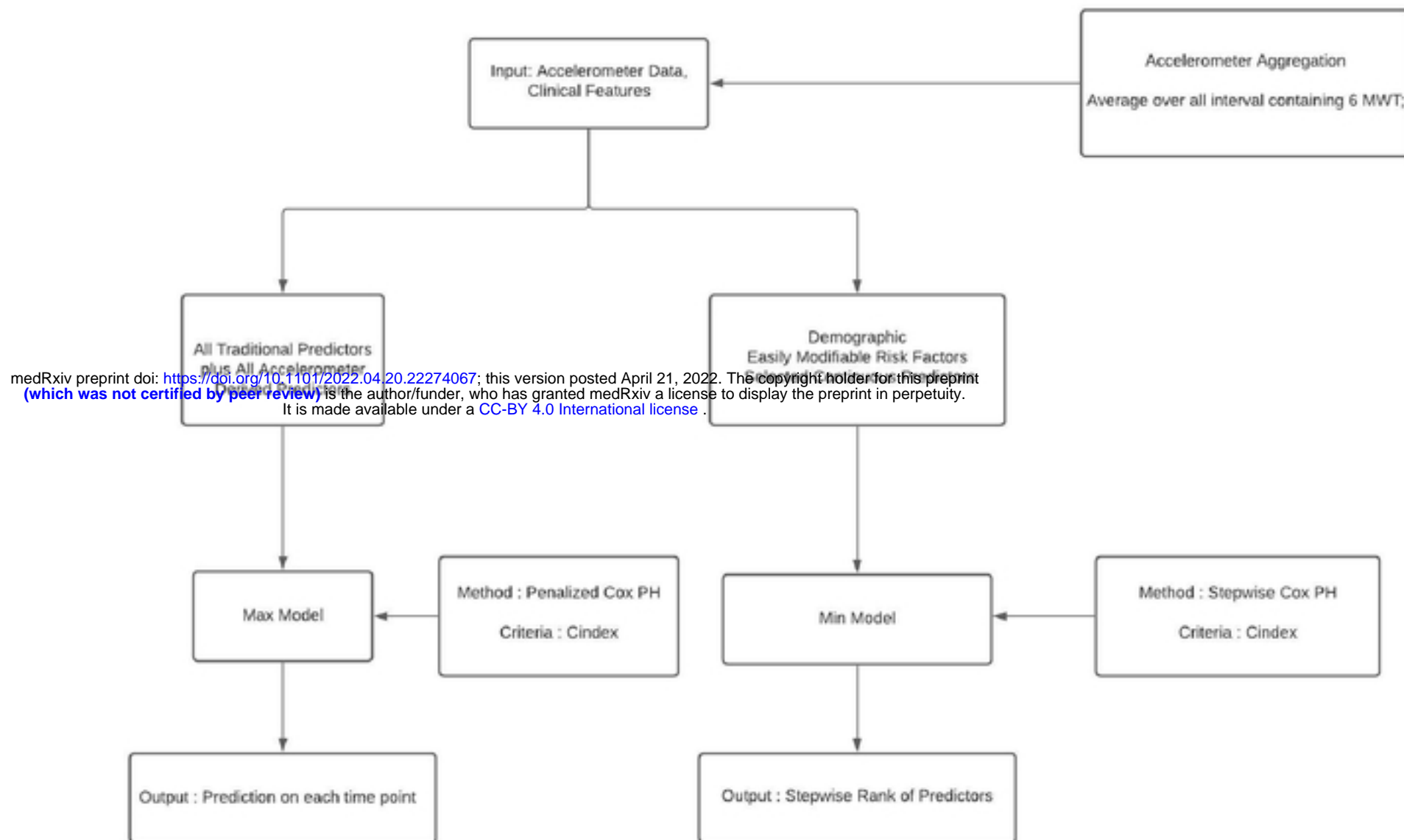
Derived Software: enmoAbs (1)

x/y/z for Min/Max, 25thp/Median/75thp, autocorr/coefvariation (21)

new features computed: RMS/TAC/MCR/MMCR +x/y/z (16)

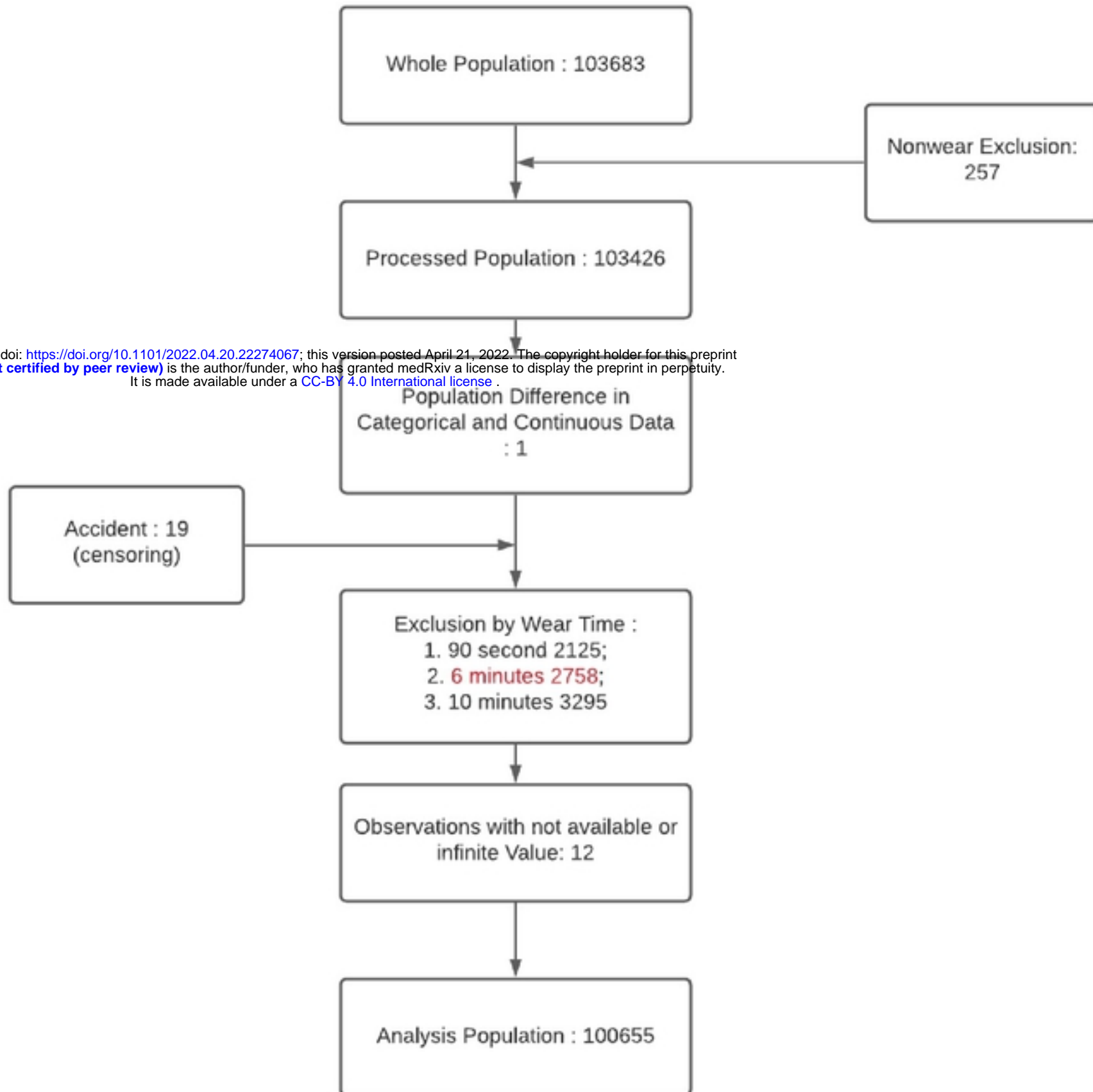
ENMOtrunc	Euclidean Norm Minus One truncated (make zero if negative)
ENMOabs	Euclidean Norm Minus One absolute (make positive if negative)
Mean	mean of vector magnitude (+x/y/z axis)
Sd	standard deviation of vector magnitude (+x/y/z axis)
RMS	Root Mean Square (quadratic mean, average power) (+x/y/z axis)
TAC	Total Activity Count (total motion amount) (+x/y/z axis)
MCR	Mean Crossing Rate (across signal average) (+x/y/z axis)
MMCR	Average of Min-Max Crossing Rate (+x/y/z axis)
MAD / MPD	Mean Amplitude Deviation / Mean Power Deviation
Min / Max	Minimum / Maximum of vector magnitude (+x/y/z axis)
	25thp/Median/75thp
Range	total range of x/y/z axis
kurt/skew	kurtosis / skewness (shape of distribution)
CoV	CoVariance in xy/xz/yz axis
corr	Correlation in xy/xz/yz axis
autocorr	autocorrelation of acceleration (time series) (+x/y/z axis)
coefvariation	coefficient of variation (relative dispersion) (+x/y/z axis)
pitchg/rollg/yawg	magnitude (gravity) of accelerometer rotation (3D)
sdpitch/sdroll/sdyaw	standard deviation of accelerometer sensor rotation
avgpitch/avgroll/avgyaw	average of accelerometer sensor rotation

Figure 1. Flowchart of Model Computation for Max and for Min Models.



medRxiv preprint doi: <https://doi.org/10.1101/2022.04.20.22274067>; this version posted April 21, 2022. The copyright holder for this preprint (which was not certified by peer review) is the author/funder, who has granted medRxiv a license to display the preprint in perpetuity. It is made available under a [CC-BY 4.0 International license](https://creativecommons.org/licenses/by/4.0/).

Figure 2. Flowchart of Participant Inclusion/Exclusion for Mortality Analysis.



medRxiv preprint doi: <https://doi.org/10.1101/2022.04.20.22274067>; this version posted April 21, 2022. The copyright holder for this preprint (which was not certified by peer review) is the author/funder, who has granted medRxiv a license to display the preprint in perpetuity. It is made available under a [CC-BY 4.0 International license](https://creativecommons.org/licenses/by/4.0/).

Figure 3a/b. Max Model for Mortality Risk.

Demo is Demographics of age/sex/race.

Cont is Continuous (Sensor) Features.

MRF is Modifiable Risk Factors (Categorical) Features,

ADC is Advanced Disease Condition (Categorical) Features.

medRxiv preprint doi: <https://doi.org/10.1101/2022.04.20.22274067>; this version posted April 21, 2022. The copyright holder for this preprint (which was not certified by peer review) is the author/funder, who has granted medRxiv a license to display the preprint in perpetuity. It is made available under a [CC-BY 4.0 International license](https://creativecommons.org/licenses/by/4.0/).

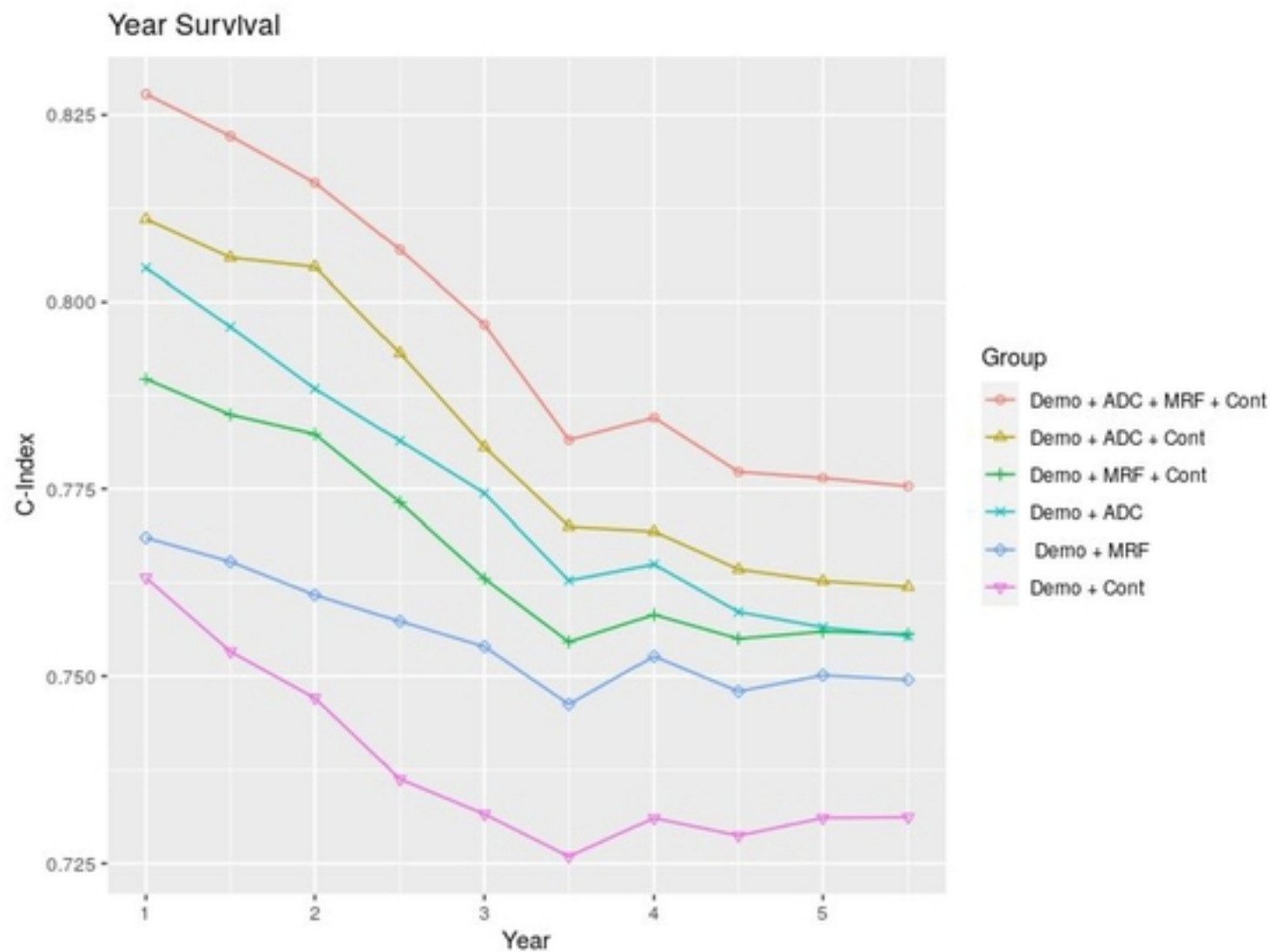
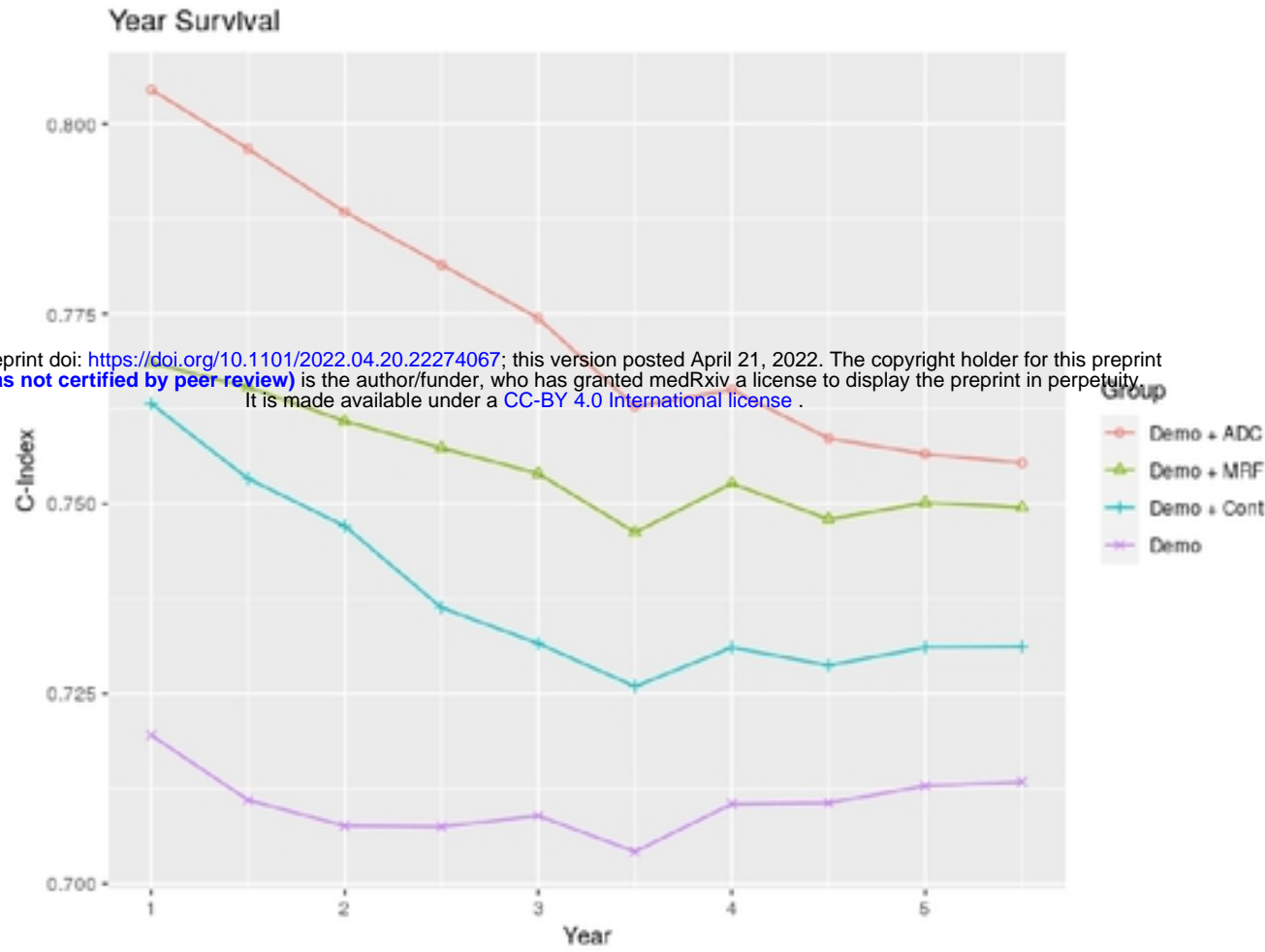


Table 3. C-index Results from Max Model. Feature Sets versus Risk Years.

FeatureSet / RiskYear	1	1.5	2	2.5	3	3.5	4	4.5	5
Demographics	0.720	0.711	0.708	0.707	0.709	0.704	0.710	0.711	0.713
advanced_disease	0.748	0.745	0.739	0.723	0.714	0.703	0.699	0.690	0.682
risk_factor	0.720	0.726	0.715	0.711	0.702	0.693	0.694	0.686	0.687
demo + advanced_disease	0.805	0.797	0.788	0.781	0.774	0.763	0.765	0.759	0.757
demo + risk_factor	0.769	0.765	0.761	0.757	0.754	0.746	0.753	0.748	0.750
risk_factor + advanced_disease	0.794	0.796	0.785	0.776	0.760	0.747	0.747	0.736	0.732
demo + risk_factor + advanced_disease	0.822	0.815	0.806	0.798	0.791	0.779	0.780	0.774	0.772
Continuous	0.688	0.694	0.693	0.690	0.684	0.673	0.676	0.668	0.671
demo + continuous	0.783	0.781	0.781	0.776	0.732	0.726	0.731	0.729	0.731
demo + advanced_disease + continuous	0.811	0.806	0.805	0.793	0.781	0.770	0.769	0.764	0.763
demo + risk_factor + continuous	0.790	0.785	0.782	0.773	0.763	0.755	0.758	0.755	0.756
demo + advanced_disease + risk_factor + continuous	0.828	0.822	0.816	0.807	0.797	0.782	0.785	0.777	0.776

medRxiv preprint doi: <https://doi.org/10.1101/2022.04.20.22274067>; this version posted April 21, 2022. The copyright holder for this preprint (which was not certified by peer review) is the author/funder, who has granted medRxiv a license to display the preprint in perpetuity. It is made available under a [CC-BY 4.0 International license](https://creativecommons.org/licenses/by/4.0/).

Figure 4. Feature Selection. Lasso lambda versus Features impact.

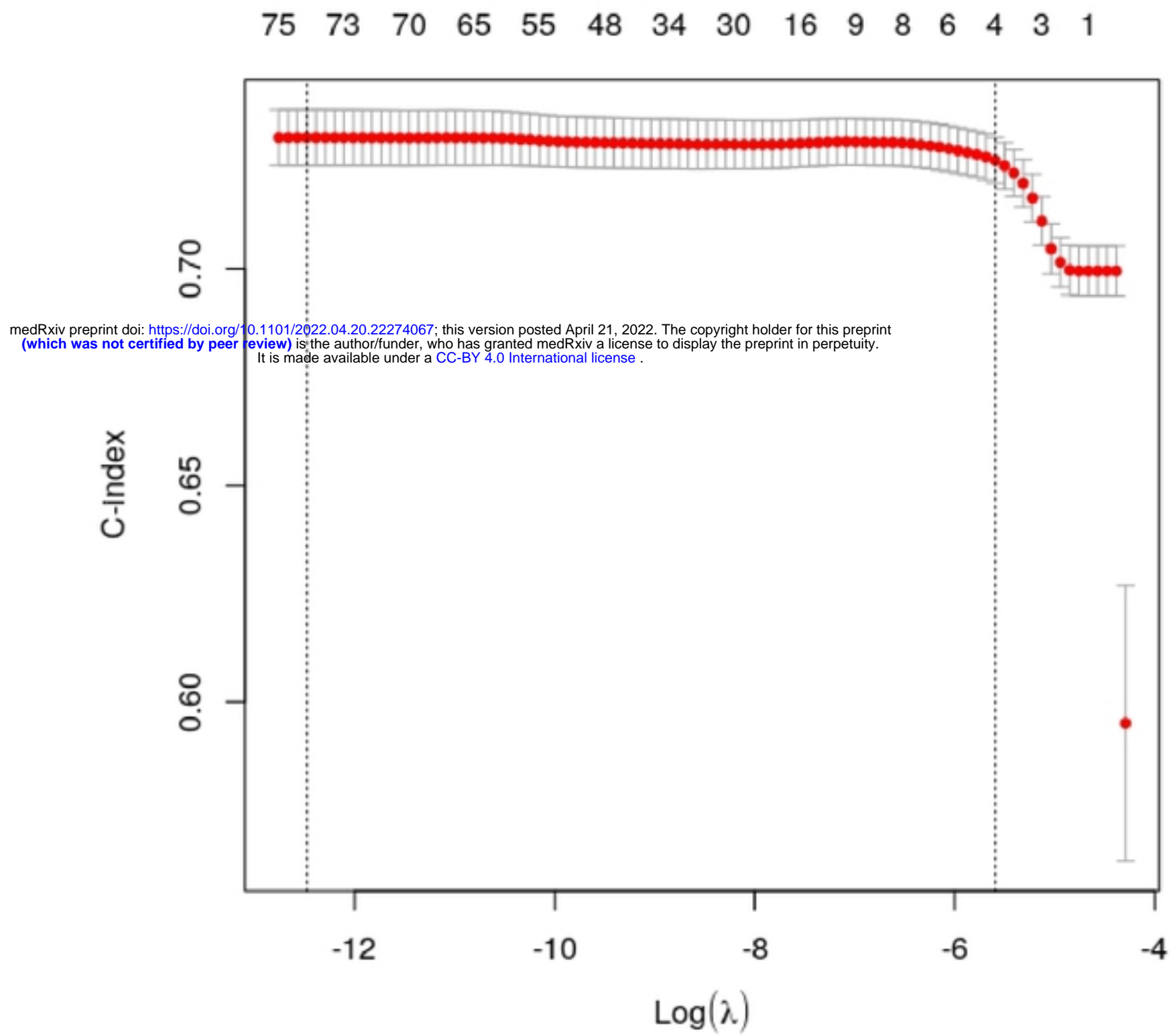


Table 4a. Min Model sensor only

No fixed features, choose top 10 most discriminating.
Includes all 76 sensor features, plus 3 demographics (age/sex/race)
Cumulative C-index for demo+continuous for 5-year risk.

	Name	Cumulative
1	Age	0.699318
2	ENMOtrunc	0.713577
3	Sex	0.727189
4	xSd	0.727784
5	Mean	0.727859
6	ySd	0.727928
7	Sd	0.728136
8	ENMOabs	0.727939
9	Race	0.727893
10	yMean	0.727674

medRxiv preprint doi: <https://doi.org/10.1101/2022.04.20.22274067>; this version posted April 21, 2022. The copyright holder for this preprint (which was not certified by peer review) is the author/funder, who has granted medRxiv a license to display the preprint in perpetuity. It is made available under a [CC-BY 4.0 International license](https://creativecommons.org/licenses/by/4.0/).

Table 4b. Min Model risk factors

No fixed features, choose top 10 most discriminating.
Includes all 76 sensor features, plus 3 demographics (age/sex/race)
Cumulative C-index for demo+continuous for 5-year risk.
Plus easy risk factors (health/obesity , smoking/alcohol)

	name	Cumulative
1	Age	0.69933
2	health	0.72245
3	Sex	0.732712
4	MPD	0.741325
5	smoking	0.745669
6	obesity	0.747336
7	zMax	0.748683
8	MAD	0.749062
9	xRMS	0.749328
10	xRange	0.749525

Figure 5. Demographic Independence Curves.

Acceleration magnitude (ENMOTrunc) independent predictor of mortality risk, against Age and Sex.

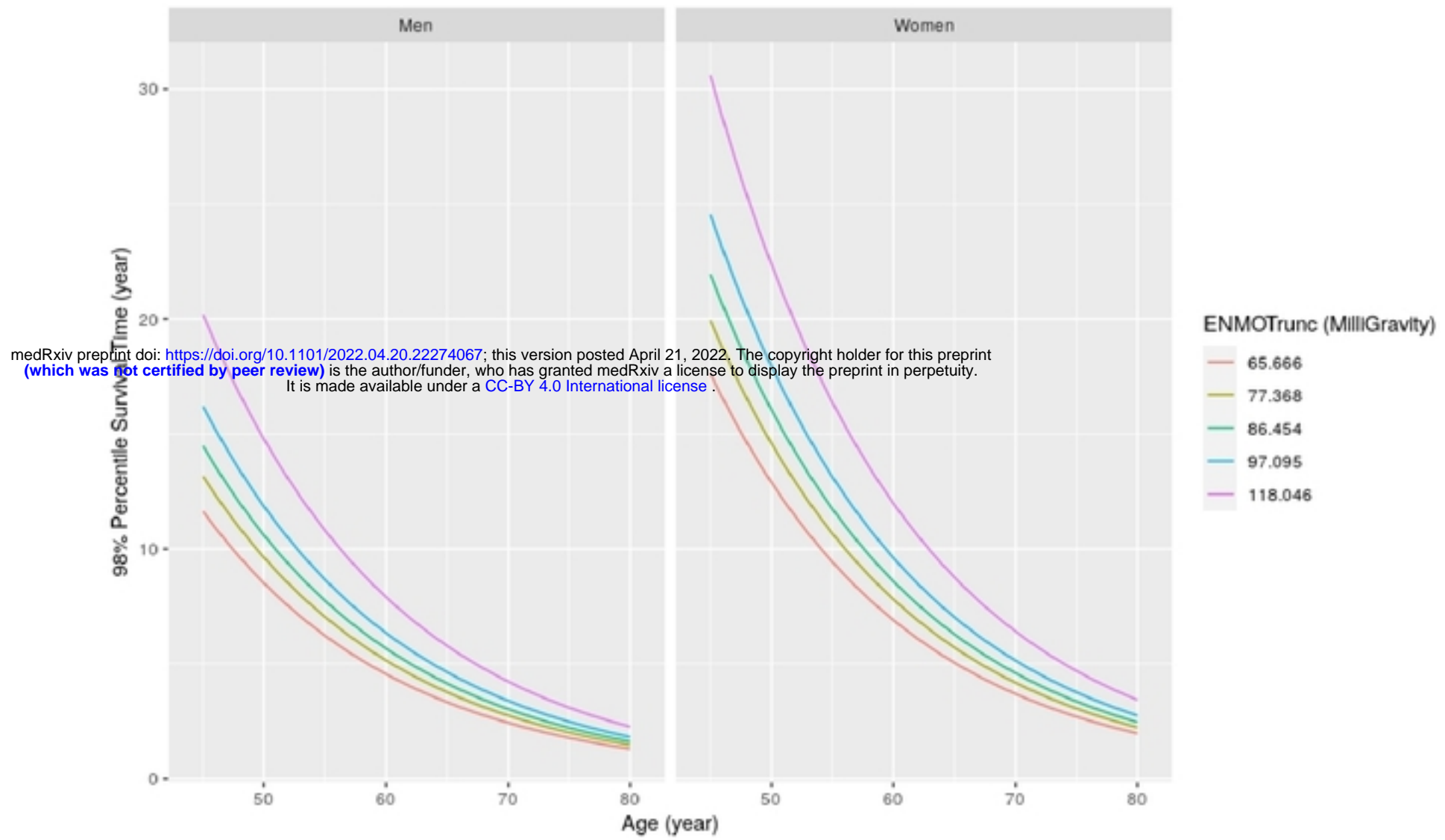
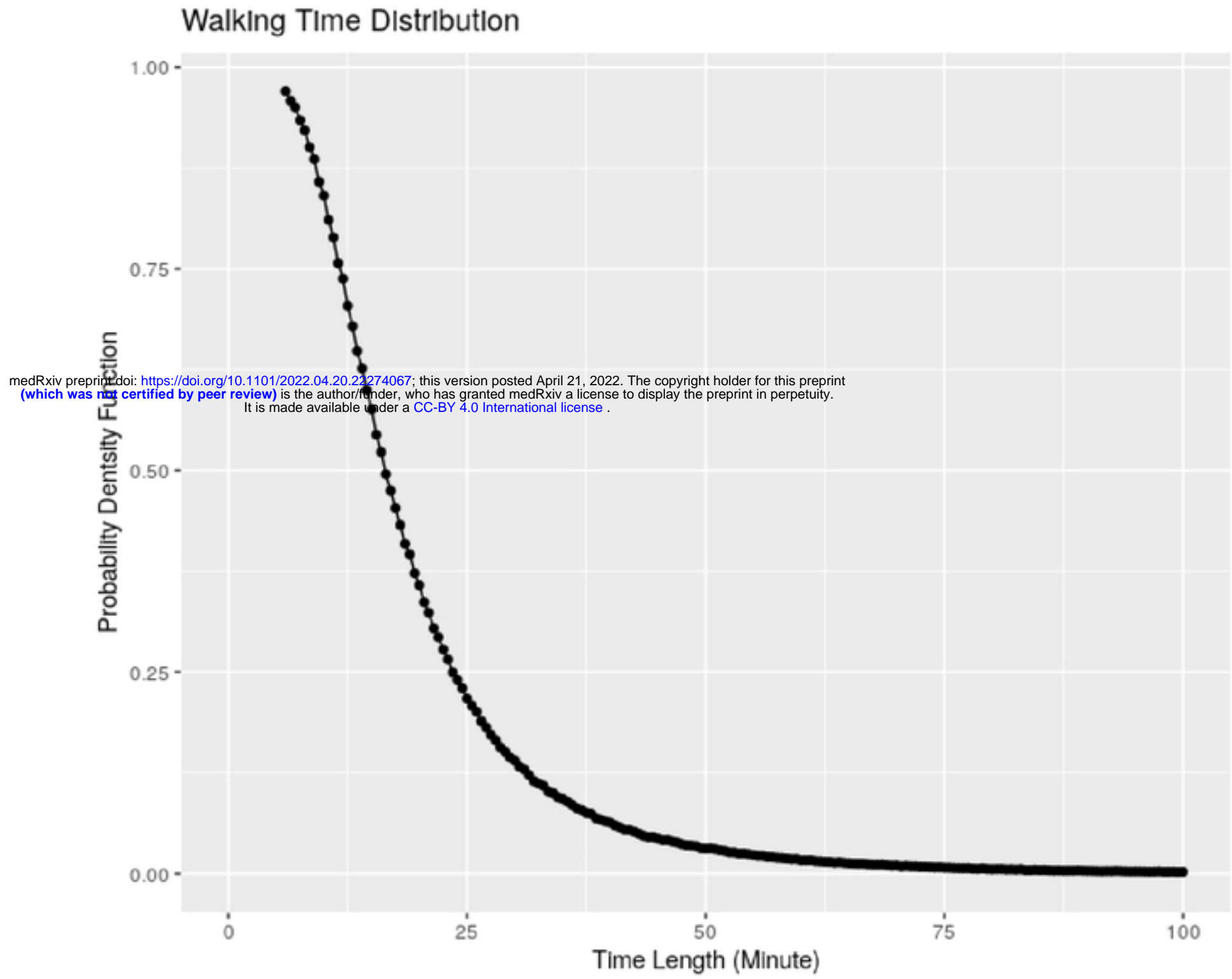


Figure 6. Walking Distribution. Steady walking session only for included participants.



SUPPLEMENTARY FIGURES/TABLES

Table S1	Categorical Encoding
Table S2	Continuous Encoding
Table S3	Marginal Performance
Figure S1	Lasso Model Features
Figure S2	Geographic Models

medRxiv preprint doi: <https://doi.org/10.1101/2022.04.20.22274067>; this version posted April 21, 2022. The copyright holder for this preprint (which was not certified by peer review) is the author/funder, who has granted medRxiv a license to display the preprint in perpetuity. It is made available under a [CC-BY 4.0 International license](#).

Table S1. Categorical Encoding of features for cohort of 100,655 participants.

Binary values are 1 for Bad (Health) and 0 for Good (Health).

Range values have more choices, specific to each such field.

For Date Fields, Censor Field if Date Report is AFTER Date Sensor, but Include Participant.

Feature_Name	Biobank_Field	Summary_Statistics
Demographics		
Age	34	DateSensorWear 90010 – YearOfBirth 34
Sex	31	(Gender) male : 43981 / female : 56674
Race	21000	(Ethnicity) others : 3493 / white : 97162
Diagnosis		
Cardiovascular Disease	8 fields	1 : 7083 / 0 : 93572 (merge w/o duplicates)
Myocardial Infarction	131298	1 : 2164 / 0 : 98491 (Date Report)
Angina Pectoris	131296	1 : 3845 / 0 : 96810 (Date Report)
Congestive Heart Failure	131354	1 : 740 / 0 : 99915 (Date Report)
Ischemic Heart Disease	131306	1 : 4248 / 0 : 96407 (Date Report)
Stroke, Cerebral Infarction	131366	1 : 441 / 0 : 100214 (Date Report)
Stroke, not Infarction	131368	1 : 1021 / 0 : 99634 (Date Report)
Stenosis, Precerebral Arteries	131370	1 : 130 / 0 : 100525 (Date Report)
Stenosis, Cerebral Arteries	131372	1 : 13 / 0 : 100642 (Date Report)
Pulmonary Disease (COPD)	42016	1 : 1685 / 0 : 98970 (Date Report)
Cancer	40005	1 : 14301 / 0 : 86354 (Date Report)
Cancer Behavior (Malignant)	40012	1 : 12825 / 0 : 87830 (Date Report)
Diabetes	3 fields	1 : 4606 / 0 : 96049 (merge w/o duplicates)
Diabetes Type1	130706	1 : 446 / 0 : 100209 (Date Report)
Diabetes Type2	130708	1 : 3389 / 0 : 97266 (Date Report)

medRxiv preprint doi: <https://doi.org/10.1101/2022.04.20.22274067>; this version posted April 21, 2022. The copyright holder for this preprint (which was not certified by peer review) is the author/funder, who has granted medRxiv a license to display the preprint in perpetuity. It is made available under a [CC-BY 4.0 International license](https://creativecommons.org/licenses/by/4.0/).

Feature_Name	Biobank_Field	Summary_Statistics
Diabetes type unspecified	130714-0.0	1 : 3237 / 0 : 97418 (Date Report)
Medicalcare		
Operation	2 fields	NAValue : 48 / Unknown : 656 / Operation : 65212 / NoOperation : 34739
Operation_male	2415	NAValue : 56697 / Unknown : 254 / Operation : 27810 / NoOperation : 15894
Operation_female	2844	NAValue : 44006 / Unknown : 402 / Operation : 37402 / NoOperation : 18845
Hospital Admission	41249	NAValue : 20471 / Emergency : 3815 / Other : 74369
Falls in last year	2296	NAValue : 45 / Unknown : 107 / High risk : 5286 / Low risk : 95217
Screening		
Hypertension	131286	1 : 15946 / 0 : 84709 (Date Report)
Cholesterol	30690	NAValue : 5892 / High : 39787 / Normal : 54976
Obesity	21001	NAValue : 226 / High : 19598 / Normal : 80831
Medications	137	NAValue : 26 / Bad : 14642 / Good : 19156 / Problem : 66831
Habit		
Alcohol	1558	NAValue : 45 / Unknown : 38 / Daily : 23025 / Week34 : 26145 / Week12 : 25228 / Month13 : 10944 / Special : 9543 / Never : 5687
Smoking	1239	NAValue : 44 / Unknown : 21 / Bad : 2239 / Sometimes : 4760 / Good : 93591
Stress	6145	NAValue : 595 / Unknown : 263 / Bad : 8287 / Serious Other : 34021 / Good : 57489
Lifestyle		
Health	2178	NAValue : 45 / Unknown : 198 / excellent : 21807 / good : 60153 / fair : 15881 / poor : 2571
Education	6138	NAValue : 594 / Unknown : 8716 / Educated : 91345
Income	738	NAValue : 704 / Unknown : 9704 / 0_18 : 13284 / 18_31 : 21798 / 31_52 : 25894 / 52_100 : 22672 / 100 : 6599

medRxiv preprint doi: <https://doi.org/10.1101/2022.04.20.22274067>; this version posted April 21, 2022. The copyright holder for this preprint (which was not certified by peer review) is the author/funder, who has granted medRxiv a license to display the preprint in perpetuity. It is made available under a CC-BY 4.0 International license.

Table S2. Continuous Encoding. Formulas for Accelerometer Derived Sensor Features.

Variable Name	Explanation	Formula
ENMOtrunc	truncated Euclidean Norm Minus One	$\max(0, \sqrt{x_i^2 + y_i^2 + z_i^2} - 1)$
ENMOabs	absolute Euclidean Norm Minus One	$ \sqrt{x_i^2 + y_i^2 + z_i^2} - 1 $
Mean (xMean, yMean, zMean)	Mean of vector magnitude (x / y / z axis)	$(\sum_{i=1}^n enmoTrunc_i) / n$ $(\sum_{i=1}^n x_i (y_i \text{ or } z_i) / n$)
Sd (xSd, ySd, zSd)	Standard deviation of vector magnitude (x / y / z axis)	$\sqrt{(\sum_{i=1}^n enmoTrunc_i - mean)^2 / n}$
RMS (xRMS, yRMS, zRMS)	Root Mean Square	$\sqrt{(\sum_{i=1}^n enmoTrunc_i^2) / n}$ $(\sqrt{(\sum_{i=1}^n x_i^2 (y_i^2 \text{ or } z_i^2) / n}$)
TAC (xTAC, yTAC, zTAC)	Total Activity	$\sum_{i=1}^n enmoTrunc_i $ $(\sum_{i=1}^n x_i (y_i \text{ or } z_i) $)
MCR (xMCR, yMCR, zMCR)	Mean Cross Rate	$(\sum_{i=1}^{n-1} 1\{ (enmoTrunc_i - mean)(enmoTrunc_i -$

medRxiv preprint doi: <https://doi.org/10.1101/2022.04.20.22274067>; this version posted April 21, 2022. The copyright holder for this preprint (which was not certified by peer review) is the author/funder, who has granted medRxiv a license to display the preprint in perpetuity. It is made available under a [CC-BY 4.0 International license](https://creativecommons.org/licenses/by/4.0/).

MMCR (xMMCR, yMMCR, zMMCR)	Maximum and Minimum Average Cross Rate	$\left(\sum_{i=1}^{n-1} 1\{ (enmoTrunc_i - (max - min)/2) (enmoTrunc_i -$
MAD	Mean Amplitude Deviation	$\left(\sum_{i=1}^n enmoTrunc_i - mean \right) / n$
MPD	Mean Power Deviation	$\left(\sum_{i=1}^n enmoTrunc_i - mean ^{1.5} \right) / n^{1.5}$
Min (xMin, yMin, zMin)	Minimum of vector	$\left(\begin{array}{l} \min_{i=1, \dots, n} enmoTrunc_i \\ \min_{i=1, \dots, n} x_i (y_i \text{ or } z_i) \end{array} \right)$
25thp (x25thp, y25thp, z25thp)	0.25 percentile	$\left(\begin{array}{l} 25\% \text{ rank of } enmoTrunc_i (i = 1, \dots, n) \\ 25\% \text{ rank of } x_i (y_i \text{ or } z_i) (i = 1, \dots, n) \end{array} \right)$
Median (xMedian, yMedian, zMedian)	median	$\left(\begin{array}{l} 50\% \text{ rank of } enmoTrunc_i (i = 1, \dots, n) \\ 50\% \text{ rank of } x_i (y_i \text{ or } z_i) (i = 1, \dots, n) \end{array} \right)$
75thp (x75thp, y75thp, z75thp)	0.75 percentile	$\left(\begin{array}{l} 75\% \text{ rank of } enmoTrunc_i (i = 1, \dots, n) \\ 75\% \text{ rank of } x_i (y_i \text{ or } z_i) (i = 1, \dots, n) \end{array} \right)$
Max (xMax, yMax, zMax)	maximum	$\left(\begin{array}{l} \max_{i=1, \dots, n} enmoTrunc_i \\ \max_{i=1, \dots, n} x_i (y_i \text{ or } z_i) \end{array} \right)$
xRange / yRange / zRange	Range of x / y / z axis	$(xmax - xmin) / (ymax - ymin) / (zmax - zmin)$

medRxiv preprint doi: <https://doi.org/10.1101/2022.04.20.22274067>; this version posted April 21, 2022. The copyright holder for this preprint (which was not certified by peer review) is the author/funder, who has granted medRxiv a license to display the preprint in perpetuity. It is made available under a [CC-BY 4.0 International license](https://creativecommons.org/licenses/by/4.0/).

Table S3. Marginal Performance. For all Features ranked by C-index.

Name	C-index
Age	0.699329
enmoTrunc	0.639477
MPD	0.637168
MAD	0.630199
enmoAbs	0.629914
Sd	0.626054
RMS	0.615782
75thp	0.612617
yRange	0.612016
Mean	0.61102
TAC	0.610951
xRange	0.61039
Ymin	0.609938
Income	0.608182
Median	0.60627
Max	0.604575
Ymax	0.603579
zRange	0.603381
Xmax	0.602969
Xmin	0.600941
Zmin	0.600338
medication	0.598063
25thp	0.597637
xRMS	0.597255
Xsd	0.59719
Zmax	0.5958
xTAC	0.590543
hypertension	0.58908
Health	0.586785
Sex	0.584188
x25thp	0.583206
x75thp	0.581649
hospital_admission	0.580935
Cancer	0.580095
Ysd	0.579393
yRMS	0.579341
Zsd	0.577168
zRMS	0.577154
yTAC	0.572009
zTAC	0.56789

medRxiv preprint doi: <https://doi.org/10.1101/2022.04.20.22274067>; this version posted April 21, 2022. The copyright holder for this preprint (which was not certified by peer review) is the author/funder, who has granted medRxiv a license to display the preprint in perpetuity. It is made available under a [CC-BY 4.0 International license](#).

ycoefvariation	0.494541
xzCov	0.492141
avgroll	0.491459
autocorr	0.49085
xcoefvariation	0.490604
yawg	0.486496
yMCR	0.484588
xmedian	0.484326
zautocorr	0.482311
yMMCR	0.478037
zMMCR	0.476288
MCR	0.47558
zMMCR	0.469512

medRxiv preprint doi: <https://doi.org/10.1101/2022.04.20.22274067>; this version posted April 21, 2022. The copyright holder for this preprint (which was not certified by peer review) is the author/funder, who has granted medRxiv a license to display the preprint in perpetuity. It is made available under a [CC-BY 4.0 International license](https://creativecommons.org/licenses/by/4.0/).

Table S3. Marginal Performance.
For all Features with C-index ranking.

Figure S1. Lasso Model. Hierarchy tree average with red selected features.

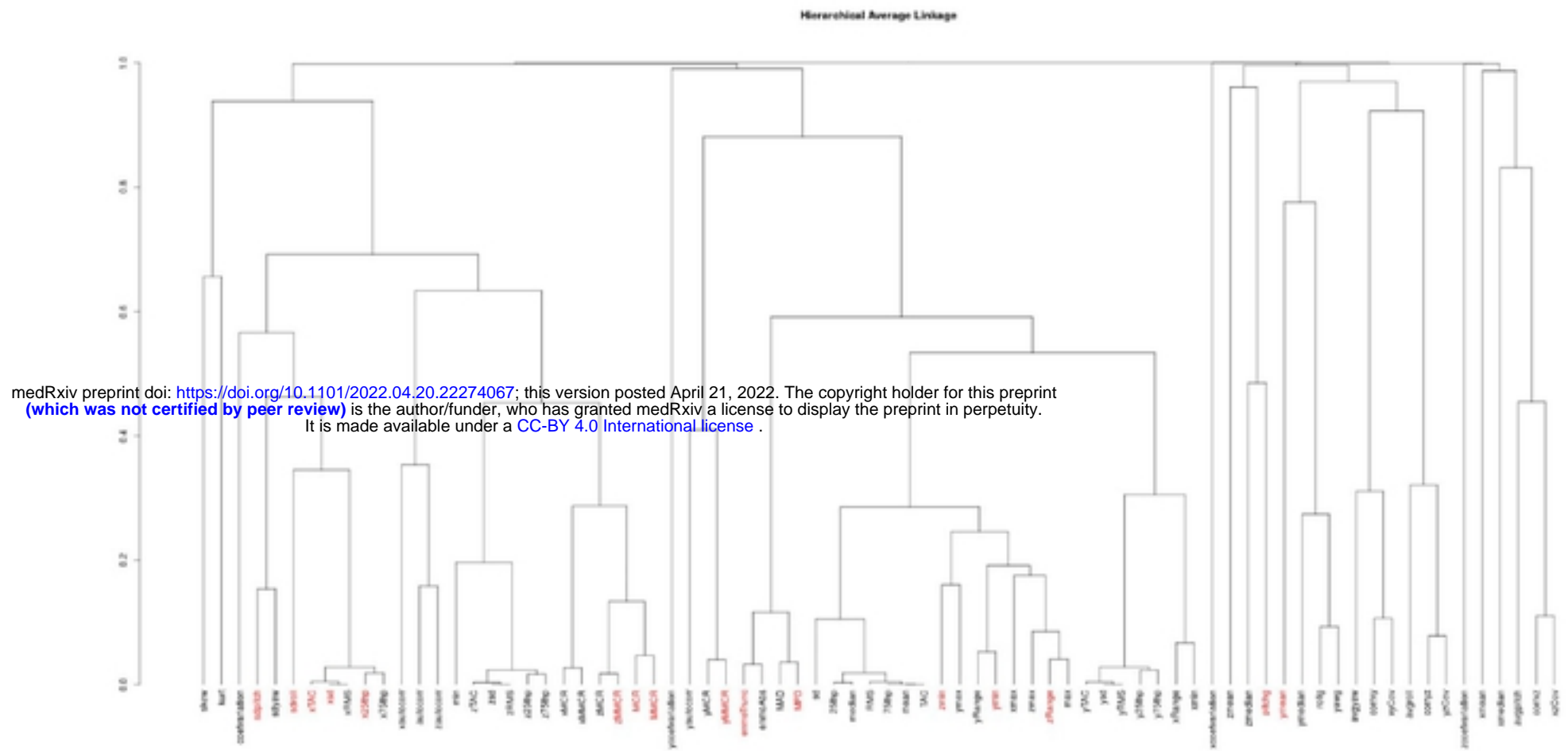


Figure S2. Geographic Models. Site by Site C-index computations.

Center Name	Center Code	Participants	Lasso Categorical	Lasso Continuous	Lasso All	Stepwise Categorical	Stepwise Continuous	Stepwise All
Manchester	11001	2595	0.78454	0.75062	0.78785	0.79374	0.73323	0.79265
Oxford	11002	3312	0.79619	0.75613	0.80127	0.79510	0.75682	0.81006
Cardiff	11003	3239	0.79595	0.74568	0.79867	0.79970	0.74584	0.80190
Glasgow	11004	2825	0.81037	0.77121	0.80908	0.80606	0.77367	0.80691
Edinburgh	11005	3882	0.80060	0.77104	0.79329	0.80185	0.77209	0.79243
Stoke	11006	2707	0.73468	0.67906	0.73819	0.72897	0.67355	0.73321
Reading	11007	7327	0.73961	0.69746	0.74270	0.73240	0.69972	0.72786
Bury	11008	4519	0.73452	0.71794	0.74684	0.73024	0.72770	0.74156
							0.70532	0.74666
Leeds	11010	8388	0.75671	0.70769	0.75936	0.75384	0.70149	0.74914
Bristol	11011	10316	0.77704	0.74624	0.78536	0.77531	0.74509	0.78368
Barts	11012	2995	0.78823	0.74812	0.79458	0.79601	0.76011	0.80440
Nottingham	11013	7171	0.72754	0.68506	0.73029	0.73535	0.68548	0.73668
Sheffield	11014	6470	0.75543	0.72846	0.76637	0.75561	0.72766	0.76419
Liverpool	11016	6079	0.77725	0.72121	0.77459	0.76850	0.72662	0.77513
Middlesborough	11017	4445	0.81426	0.77394	0.81623	0.81332	0.77326	0.81421
Hounslow	11018	7132	0.78572	0.73614	0.78352	0.78419	0.74229	0.78201
Croydon	11020	6830	0.79246	0.71938	0.79312	0.78947	0.71654	0.78011
Birmingham	11021	5484	0.80127	0.76102	0.80882	0.79677	0.75446	0.79944
Swansea	11022	482	0.78212	0.73497	0.80170	0.76685	0.73578	0.78333
Wrexham	11023	144	0.81139	0.66192	0.84342	0.81673	0.72242	0.81139
All		103425	0.77091	0.72870	0.77458	0.76872	0.72867	0.77083

medRxiv preprint doi: <https://doi.org/10.1101/2022.04.20.22274067>; this version posted April 21, 2022. The copyright holder for this preprint (which was not certified by peer review) is the author/funder, who has granted medRxiv a license to display the preprint in perpetuity. It is made available under a [CC-BY 4.0 International license](https://creativecommons.org/licenses/by/4.0/).